

crystals (yield 6.3 g, 54%). The purity of the product was confirmed by ^{13}C NMR.³³

Reactions in Sealed Glass Tubes. The polymers were heated in sealed Pyrex tubes, 220 mm long, 12-mm o.d., and 10-mm i.d., with a constriction 100 mm from the open end. The tubes were cleaned with ethanolic potassium hydroxide and were then washed in turn with tap water, 2% aqueous hydrochloric acid, and distilled deionized water. The tubes were then dried at 140 °C for 48 h. Each tube was charged with 10–15 g of polymer in a nitrogen-filled drybox and was then connected to a vacuum line for evacuation for 30 min at 0.005 Torr. The tubes were sealed at the constriction, wrapped in aluminum gauze, and placed on a rocking device in a Freas thermoregulated oven equilibrated at the required temperature. The tubes were removed from the oven, placed in a desiccator, and allowed to cool to room temperature. They were then opened under dry nitrogen within a drybox, and the contents were dissolved in THF (5–10 mL) before analysis by ^{31}P NMR spectroscopy.

Pyrolysis of the Polymers in a Tube Furnace. The polymer samples were placed in a ceramic boat, which was placed in a quartz flow tube and heated in a Linderberg 55035A tube furnace. The entire pyrolysis was carried out under a constant flow of nitrogen. The samples were heated from 25 to 1000 °C over 2 h, and fractions of the volatile byproducts were collected in a trap cooled to –196 °C. The volatile products were analyzed by gas chromatography/mass spectrometry and, when appropriate, by NMR spectroscopy.

The temperatures within the quartz tube downstream of the heated zone were measured in the following way. The tube furnace

was operated under the conditions normally employed for the pyrolysis reactions. A nitrogen flow was established at a flow rate of 50–75 mL/min, and the furnace was allowed to reach operating temperature. Temperatures within the flow tube were measured by means of a Cole Parmer Digi-Sense unit with type K thermocouple. Higher temperatures were detected near the inside wall of the tube than in the center of the gas flow, and the reaction temperatures quoted take this into account.

Thermogravimetric Analyses of the Polymer Systems. The polymer samples (1–3 mg) were analyzed under a constant flow of nitrogen in platinum pans at a heating rate of 2 °C/min with an initial temperature of 50 °C and a final temperature of 1000 °C. The instrument was calibrated by using the magnetic standards alumel (163 °C), nickel (354 °C), and peralloy (596 °C) samples.

Thermally Induced Cyclopentadienyl Ligand Exchange between $\text{Fe}(\eta\text{-C}_5\text{H}_5)_2$ and $\text{Fe}(\eta\text{-C}_5\text{H}_4\text{Me})_2$. A solid mixture of $\text{Fe}(\eta\text{-C}_5\text{H}_5)_2$ (0.64 g, 3.44 mmol) and $\text{Fe}(\eta\text{-C}_5\text{H}_4\text{Me})_2$ (0.74 g, 3.46 mmol) was placed in a thick-walled Pyrex glass tube that was then cooled to –196 °C, sealed under vacuum (0.002 mmHg), and heated to 250 °C. After 14 days the contents of the tube were dissolved in CDCl_3 (5 mL) and were analyzed by high-field ^{13}C NMR spectroscopy. The product mixture consisted of the ligand-exchanged product $\text{Fe}(\eta\text{-C}_5\text{H}_4\text{Me})(\eta\text{-C}_5\text{H}_5)$ ³³ (ca. 60%) and the starting materials (each ca. 20%).

^{31}P Chemical Shifts Used for Product Identification. The ^{31}P NMR shifts (in parentheses) were as follows: $[\text{NP}(\text{OCH}_2\text{CF}_3)_2]_n$, $n = 10\text{--}15\,000$ (–7.9 ppm), $n = 3$ (+17.0 ppm), $n = 4$ (–2.0 ppm).

Acknowledgment. We thank the U.S. Air Force Office of Scientific Research for support of this work. We also thank R. Minard for the GC/mass spectrometry analyses.

(33) Braun, S.; Abram, T. S.; Watts, W. E. *J. Organomet. Chem.* 1975, 97, 429.

Metallaboranes as Molecular Precursors to Thin Metal–Boride Films. Conversion of $\text{HFe}_3(\text{CO})_9\text{BH}_4$ to Amorphous $\text{Fe}_{75}\text{B}_{25}$

Mostafa M. Amini and Thomas P. Fehlner*

Department of Chemistry, University of Notre Dame, Notre Dame, Indiana 46556

Gary J. Long* and Mark Politowski

Department of Chemistry, University of Missouri—Rolla, Rolla, Missouri 65401

Received April 5, 1990

The thermal decomposition of $\text{HFe}_3(\text{CO})_9\text{BH}_4$ on glass or aluminum substrates at 175–200 °C at pressures between 10^{-5} and 10^{-4} Torr results in the deposition of uniform, amorphous alloy films of approximate composition $\text{Fe}_{75}\text{B}_{25}$ with individual film thicknesses ranging from 1000 to 10 000 Å. The glassy metal films have been characterized by Auger, X-ray, and Mössbauer spectroscopies. The Mössbauer spectra show that the local structure of the film is similar to that observed for films prepared by rapid quenching techniques. In contrast, magnetically ordered films prepared from $\text{HFe}_3(\text{CO})_9\text{BH}_4$ exhibit magnetic moments having a preferential orientation normal to rather than parallel with the film plane. Although the films are stable in air, oxidation during deposition readily takes place under poor vacuum conditions and leads to films containing oxidized boron. The stoichiometry of the oxide phase has been shown to be B_2O_3 (oxygen content 3–11%). The film resistivity increases with increasing oxygen content.

Introduction

Chemical vapor deposition (CVD) is a well-established methodology for the production of materials from molecular precursors.¹ In the early and current use of this

method, appropriate mixtures of small molecules containing the elements of interest are used. Recently it has been recognized that there are advantages to using sophisticated molecular precursors for the generation of solid-state materials. These advantages include milder deposition conditions, higher purities, better stoichiometry control, and better kinetic control of product formation. Hence, organic and inorganic chemists have become in-

(1) Powell, C. F.; Oxley, J. H.; Blocher, J. M. *Vapor Deposition*; Wiley: New York, 1966.

volved in the synthesis of molecular precursors for a variety of materials.²

Amorphous alloys containing transition-metal and main-group atoms, often referred to as metallic glasses, constitute advanced materials of much interest.³ Metal borides, e.g., $\text{Fe}_{80}\text{B}_{20}$, were among the earliest of such materials to be explored.⁴ These are now prepared on a large scale by rapid quenching and melt-spinning methods. We have prepared and characterized a number of ferraboranes that can, in principle, serve as molecular precursors to thin alloy films containing iron and boron. Some of these volatile metallaboranes have cluster core stoichiometries corresponding to known metallic glasses, e.g., the core composition of $\text{HFe}_4(\text{CO})_{12}\text{BH}_2$ corresponds to $\text{Fe}_{80}\text{B}_{20}$, and hence we have begun a study to determine whether this class of compounds can serve as molecular precursors. Although molecular precursors have an obvious economic disadvantage for the preparation of bulk materials, there are clear advantages for specialized applications. For example, deposition under mild conditions can be carried out on fragile, complex substrates to avoid problems in fabrication. Further, a single precursor permits the determination of the material stoichiometry by the precursor composition. Finally, most borides are formed under rigorous conditions such that only the thermodynamically favored product is formed. An approach via readily converted molecular precursors both permits access to known materials and also, in principle, permits the formation of these materials with different properties. Of course materials presently inaccessible via known techniques are also potential goals for the molecular precursor approach.

Our initial study, in which $\text{HFe}_4(\text{CO})_{12}\text{BH}_2$ was converted into $\text{Fe}_{80}\text{B}_{20}$, has already been reported.⁵ Evidence was presented for the formation of authentic $\text{Fe}_{80}\text{B}_{20}$, but the low-pressure pyrolysis technique used also created problems. The main problem was oxidation, which took place concurrently with deposition. In this work we report the utilization of $\text{HFe}_3(\text{CO})_9\text{BH}_4$ as a precursor for the formation of thin films of $\text{Fe}_{75}\text{B}_{25}$. We also report a so-

(2) Aylett, B. J.; Colquhoun, H. M. *J. Chem. Soc., Dalton* 1977, 2058. Aylett, B. J.; Tannahill, A. A. *Vacuum* 1985, 35, 435. Girolami, G. S.; Jensen, J. A.; Pollina, D. M.; Williams, W. S.; Kaloyer, A. E.; Allocacca, C. M. *J. Am. Chem. Soc.* 1987, 109, 1579. Kaloyer, A. E.; Williams, W. S.; Allocacca, C. M.; Pollina, D. M.; Girolami, G. S. *Adv. Ceram. Mater.* 1987, 2, 257. Jensen, J. A.; Gozum, J. E.; Pollina, D. M.; Girolami, G. S. *J. Am. Chem. Soc.* 1988, 110, 1643. Jefferies, P. M.; Girolami, G. S. *Chem. Mater.* 1989, 1, 8. Czekaj, C. L.; Geoffroy, G. L. *Inorg. Chem.* 1988, 27, 8. Bochmann, M.; Hawkins, I.; Wilson, L. M. *J. Chem. Soc., Chem. Commun.* 1988, 344. Wayda, A. L.; Schneemeyer, L. F.; Opila, R. L. *Appl. Phys. Lett.* 1988, 53, 361. Steigerwald, M. L.; Rice, C. E. *J. Am. Chem. Soc.* 1988, 110, 4228. Steigerwald, M. L. *Chem. Mater.* 1989, 1, 52. Boyd, D. C.; Haasch, R. T.; Mantell, D. R.; Schulze, R. K.; Evans, J. F.; Gladfelter, W. L. *Chem. Mater.* 1989, 1, 119. Cowley, A. H.; Benac, B. L.; Ekerdt, J. G.; Jones, R. A.; Kidd, K. B.; Lee, J. Y.; Miller, J. E. *J. Am. Chem. Soc.* 1988, 110, 6248. Gross, M. E.; Jasinski, J. M.; Yates, J. T., Jr., Eds. *Chemical Perspectives of Microelectronic Materials: Materials Research Society*: Pittsburgh, PA, 1989. Interrante, L. V.; Carpenter, L. E., II; Whitmarsh, C.; Lee, W.; Garbauskas, M.; Slack, G. A. *Mater. Res. Soc. Symp. Proc.* 1986, 73, 359. Seyforth, D.; Wiseman, G. H. In *Ultrastructure Processing of Ceramics, Glasses, and Composites*; Hench, L. L.; Ulrich, D. R., Eds.; Wiley: New York, 1984; p 265. Dowben, P. A.; Spencer, J. T.; Stauff, G. T. *Mater. Sci. Eng.* 1989, B2, 297. Kim, Y. G.; Dowben, P. A.; Spencer, J. T.; Ramseier, G. O. *J. Vac. Sci. Technol. A* 1989, 7, 2796. Stauff, G. T.; Dowben, P. A.; Emrich, K.; Barfuss, S.; Hirschwald, W.; Boag, N. M. *J. Phys. Chem.* 1989, 93, 749. Cowley, A. H.; Jones, R. A. *Angew. Chem., Int. Ed. Engl.* 1989, 28, 1208.

(3) Hasegawa, R., Ed. *Glassy Metals: Magnetic, Chemical and Structural Properties*; CRC Press: Boca Raton, FL, 1983.

(4) Hasegawa, R.; O'Handley, R. C.; Tanner, L. E.; Ray, R.; Kavesh, S. *Appl. Phys. Lett.* 1976, 29, 219.

(5) Fehlner, T. P.; Amini, M. M.; Zeller, M. V.; Stickle, W. F.; Pringle, O. A.; Long, G. J.; Fehlner, F. P. In *Chemical Perspectives of Microelectronic Materials*; Gross, M. E.; Jasinski, J. M.; Yates, J. T., Jr., Eds.; Materials Research Society: Pittsburgh, PA, 1989; p 413.

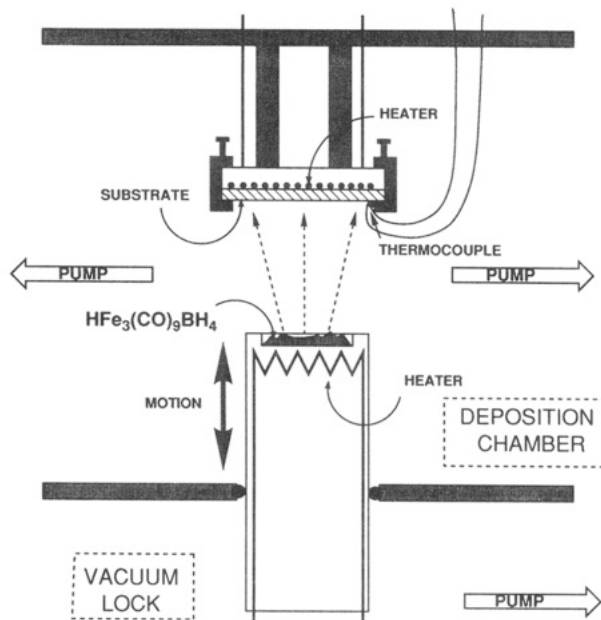


Figure 1. Schematic diagram of deposition apparatus. The precursor can be admitted into the deposition chamber via the vacuum lock without appreciable deterioration of the vacuum.

lution to the oxidation problem experienced earlier.

Experimental Section

The $\text{HFe}_3(\text{CO})_9\text{BH}_4$ cluster⁶ was prepared according to a new procedure⁷ by the reaction of $[\text{Fe}_4(\text{CO})_{13}]^{2-}$ with $\text{BH}_3\text{-THF}$ and was purified by recrystallization from hexanes. To prepare a film, the $\text{HFe}_3(\text{CO})_9\text{BH}_4$ was sublimed at 22 °C in the low-pressure CVD reactor shown schematically in Figure 1. To eliminate the sulfur contamination found with the earlier system,³ the reactor was sealed, with two exceptions, with copper gaskets. Heating overnight to 60–70 °C reduced the water vapor to workable levels ($\approx 2 \times 10^{-9}$ Torr). The position of the precursor sublimation cup relative to the substrate surface could be easily adjusted from outside the vacuum chamber. For most depositions the cup was positioned 2–4 cm below the substrate surface. For the same sample charge, the shorter distance gave thicker films, while the longer distance gave films of more uniform thickness over the entire substrate. Typical deposition times were 15–20 min. The substrates were resistively heated to a temperature of 160–180 °C and monitored by a 0.005-in.-diameter iron/constantan thermocouple held in place on the outer face of the substrate surface by the substrate-heater clamp. The temperature measured by the thermocouple increased 5–10 °C during the deposition of the highly reflective film. This was a convenient, if phenomenological, method for monitoring the onset and initial growth of the film. The reactor was evacuated with a turbomolecular pump and ion pump, and a base pressure of 2×10^{-8} Torr was achieved after heating overnight at ≈ 60 °C. During deposition, total pressures initially were $\approx 10^{-4}$ Torr and decreased to 10^{-5} Torr as the solid sample sublimed away.

The glass substrates (Corning 7059, 2 × 2.5 cm) were cleaned with soap and rinsed with distilled water, acetone, and ethanol. This treatment was followed by heating at 550 °C for several hours in air before deposition. Deposition was also carried out on iron-free aluminum foil covering a glass substrate for the Mössbauer studies. The ceramic and stainless steel parts of the deposition apparatus at elevated temperatures were also coated with the film.

Film thicknesses were measured with a Tencor profilometer. The extent of crystallinity was assayed with a Nicolet I2 X-ray powder diffraction system. Film composition was determined by elemental analysis, Auger, and Mössbauer spectroscopy. Auger

(6) Vites, J. C.; Eigenbrot, C.; Fehlner, T. P. *J. Am. Chem. Soc.* 1984, 106, 4633. Vites, J. C.; Housecroft, C. E.; Eigenbrot, C.; Buhl, M. L.; Long, G. J.; Fehlner, T. P. *J. Am. Chem. Soc.* 1986, 108, 3304.

(7) Meng, X.; Fehlner, T. P. *Inorg. Synth.*, submitted.

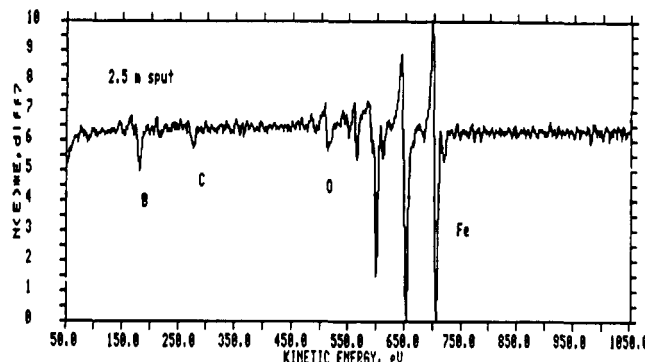


Figure 2. Auger spectrum ($dN(E)/E$) obtained at 10 kV of a $\text{Fe}_{75}\text{B}_{25}$ film after sputtering ≈ 700 Å of the top surface of a 3600-Å thick film on a glass substrate. Acquisition time was ca. 5 min. and total C + O is ≈ 10 at. %. The low sensitivity for boron relative to the other elements is evident.

spectra were obtained on a Perkin-Elmer 660 scanning Auger Multiprobe with 5- or 10-kV electrons after sputtering with 5-kV Ar^+ (1 mm^2 spot) to constant composition (≤ 200 Å). Beam currents of 6 nA were generally used, and little reduction of any oxides in the film was observed. Standard instrument sensitivities were used to obtain compositions. The Mössbauer effect spectra were obtained at 296 and 78 K on a constant acceleration spectrometer that utilized a room-temperature rhodium matrix ^{57}Co source and was calibrated at room temperature with natural-abundance α -iron foil. The Mössbauer spectra were fit by two different methods. In the first, the spectra were fit with a magnetic sextet and two symmetric doublets with Lorentzian line-shape components. In these fits the areas of the sextet components were constrained in the ratio of $3:x:1:1:x:3$ and the line widths of the components were constrained in the ratio of $\Gamma + \Delta\Gamma:\Gamma + 0.5\Delta\Gamma:\Gamma:0.5\Delta\Gamma:\Gamma + \Delta\Gamma$, where $\Delta\Gamma$ was determined from the preliminary fits. In the second method,⁸ the spectra were fit to a distribution of hyperfine fields with a single isomer shift, quadrupole shift, and line width, and for a fixed value of x , the intensity of the two and five lines. Because these distribution fits can be carried out only for a single isomer shift, the high-spin iron(II) component with 3% and 5% of the total area at 296 and 78 K were subtracted from the data for these fits.

Results

Film Preparation and Characterization. As is evidenced by the mass spectrum obtained in the gas phase, $\text{HFe}_3(\text{CO})_9\text{BH}_4$ vaporizes as a molecular species.⁹ Exposure in the LPCVD reactor of a glass substrate at 175 °C to $(1-10) \times 10^{-5}$ Torr of $\text{HFe}_3(\text{CO})_9\text{BH}_4$, produced by the sublimation of a 20–30-mg crystalline sample held at 22–25 °C for 15–30 min, results in the formation of a film on the glass substrate with a metallic appearance and a smooth, mirrorlike surface. Direct pyrolysis of the broad molecular beam emanating from the precursor crucible on the substrate surface was demonstrated by noting the decrease in film thicknesses with increasing radial distance from the crucible axis. Consistent with this observation, a decreasing film thickness with increasing crucible to substrate distance for a fixed deposition time and crucible temperature was also noted. Further, for a given precursor sublimation rate, the total pressure in the chamber increased as the crucible to substrate distance decreased. This reflects an increased production of CO and H_2 and a greater pyrolysis efficiency at shorter distances. These observations indicate a substantial amount of direct decomposition of $\text{HFe}_3(\text{CO})_9\text{BH}_4$ on the surface of the substrate and a low mobility of the surface species which leads to film for-

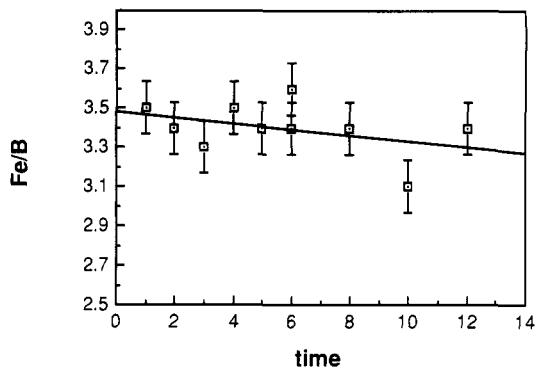


Figure 3. Plot of Fe/B (atom per cents derived from Auger spectra) vs sputtering time (5 kV at $1 \times 1 \text{ mm}^2$) for a 10000-Å film demonstrating invariance of composition with depth and sputtering time. The total depth sputtered away at 12 min as measured by profilometry is 3600 Å.

mation. The films adhere well to glass as judged by the "Scotch tape test". Film thicknesses varied from 1000 to 10000 Å depending on sample size, crucible-to-substrate distance, and deposition time.

A typical Auger spectrum of a film formed from $\text{HFe}_3(\text{CO})_9\text{BH}_4$ is shown in Figure 2. The surface of the films were highly oxidized and sputtering with argon ions was necessary to remove this surface contamination. In an earlier electron spectroscopic study of iron borides¹⁰ it was reported that, after sputtering for equal times, borides of the known bulk compositions FeB and Fe_2B reached equal surface compositions of approximately Fe_5B . The authors concluded that boron sputters preferentially and that composition measurements carried out after such treatment will be skewed toward a high iron content. To investigate the extent of preferential sputtering in our films, we measured the Fe/B atom ratio as a function of sputtering time with the result as shown in Figure 3. Under our sputtering conditions, the ratio of Fe/B is constant within experimental error up to a depth of 3600 Å. Indeed, if anything, the ratio decreases slightly with increased sputtering. It is possible that our sputtering conditions are milder than those used earlier as we see only traces of implanted argon atoms in our films, but in any case it is clear that sputtering does not appreciably change the boron-to-iron ratio in our samples. It is also possible that the composition measurements can be distorted by the reduction of surface oxides by the electron beam, thereby underestimating the extent of oxidation. However, the fact that we are able to observe oxidation of the film *in situ* (see below) suggests that such reduction is not a significant factor at the low beam currents employed in our work.

Auger spectroscopy, with standard instrument sensitivities, was used to analyze films of thicknesses from 1000 to 10000 Å prepared at temperatures ranging from 175 to 220 °C and gave Fe/B ratios of 3.4 ± 0.3 and C and O impurities of ≤ 5 and 3 at. %, respectively, when the films were prepared under the most rigorous conditions. Several locations on the film surface were examined with no significant difference in the observed composition. The composition also appeared uniform with depth. The apparent Fe/B ratio is high compared to the expected ratio of 3.0 if the cluster core is indeed incorporated intact into the film. Chemical analysis of the entire film by inductively coupled plasma emission spectroscopic analysis of a solution resulting from dissolving the film in perchloric

(8) Wivel, C.; Morup, S. *J. Phys. E: Sci. Instrum.* 1981, 14, 605.
(9) Vites, J. C. Ph.D. Thesis, University of Notre Dame, Notre Dame, IN, 1984.

(10) Joyner, D. J.; Johnson, O.; Hercules, D. M. *J. Am. Chem. Soc.* 1980, 102, 1910.

Table I. Mössbauer Parameters of a $\text{Fe}_{75}\text{B}_{25}$ Film Deposited on Aluminum

| T, K | H, kOe | δ , ^a mm/s | QS, ^b mm/s | Γ , mm/s | $\Delta\Gamma$, mm/s | $\langle\theta\rangle$, deg | x ^c | area, ^d % |
|------|-------------------------|------------------------------|-----------------------|-----------------|-----------------------|------------------------------|------------------|----------------------|
| 296 | 220 ^e | 0.18 | -0.10 | 0.52 | 1.06 | 28 | 0.50 | 87 |
| | 0 ^f | 0.24 | 0.65 | 0.68 | | | | 13 |
| 78 | 237 ^e | 0.29 | -0.14 | 0.62 | 1.21 | 29 | 0.53 | 94 |
| | 0 ^f | 0.08 | 1.02 | 0.41 | | | | 6 |
| 296 | $\langle 178 \rangle^g$ | 0.22 | 0.00 | 0.45 | 29 | 0.50 | 100 | |
| | $\langle 206 \rangle^g$ | 0.27 | 0.00 | 0.39 | | | | 100 |

^aThe isomer shift is relative to room temperature natural α -iron foil. ^bQS is the quadrupole shift for the sextets and the quadrupole splitting for the doublets. ^cThe areas of the components of the sextets was constrained to $3:x:1:1:x:3$, where x is the area of the 2 and 5 line.

^dThe spectra also contain between 3 and 5% of a paramagnetic high-spin iron(II) component. Type of fit: ^ehexet; ^fdoublet; ^g $P(H)$.

acid yielded a ratio of Fe/B of 3.87, which again is higher than expected. Although the high ratio may be due to systematic errors in the analyses, the loss of boron via a volatile borane during deposition could also account for the high ratio. To obtain a better insight into the reliability of the measured values of the Fe/B ratio, we compared data obtained on two films prepared by the deposition of $\text{HFe}_3(\text{CO})_9\text{BH}_4$ and $\text{HFe}_4(\text{CO})_{12}\text{BH}_2$ under similar conditions. Auger analysis was carried out on side by side films under identical spectrometer operating conditions. The ratio of Fe/B ratios for the two compounds was 1.27 ± 0.2 (four determinations) vs the 1.33 expected ratio. This indicates that, in going from $\text{HFe}_3(\text{CO})_9\text{BH}_4$ to $\text{HFe}_4(\text{CO})_{12}\text{BH}_2$, the film does become richer in iron by the amount expected on the basis of the stoichiometry of the cluster cores. Although these analyses do not fix the absolute Fe/B ratio for the deposition of $\text{HFe}_3(\text{CO})_9\text{BH}_4$ with the precision desirable, it is probable that the material is $\text{Fe}_{75}\text{B}_{25}$. The Mössbauer spectra, see below, support this conclusion.

The lines observed in the Auger spectrum ($dN(E)/E$) appeared at kinetic energies of 704, 180, 513, and 274 eV for Fe, B, O, and C, respectively. These values are consistent with those reported earlier³ for films deposited from $\text{HFe}_4(\text{CO})_{12}\text{BH}_2$ as well as from other borides.⁶ Hence, as the Auger lines are sensitive to surroundings, the chemical environments of the boron and iron atoms in our films are similar to those of known borides. Note, however, that the Auger energies are not sensitive enough to distinguish α -Fe from iron in a boride phase.

The X-ray diffraction study of the thin film deposited on glass shows only broad peaks, which may be attributed to the glass substrate. Clearly the overall structure of the material in the film is amorphous in nature. As an α -iron phase of 50% abundance has been detected previously¹¹ in nitride films of $\approx 500\text{-}\text{\AA}$ thickness, we can conclude that the abundance of α -iron in this sample is $\leq 2.5\%$. A crude estimate of film smoothness was obtained with a profilometer. In a typical scan of a $10\,000\text{-}\text{\AA}$ film, the surface showed broad "hills and valleys" of amplitude of $\approx 200\text{ \AA}$, upon which was superimposed a higher frequency noise with a RMS amplitude of $\approx 200\text{ \AA}$. There was typically a low density (1 per mm^2) of holes ($\approx 2000\text{ \AA}$ wide) in the film.

The resistivity was measured for a uniform film of $1.5\text{ cm} \times 0.6\text{ cm} \times 1000\text{ \AA}$, which was deposited through a mask on a glass substrate upon which an equally spaced array of four chromium electrodes had previously been deposited. Resistivity measurements by the four-point probe method¹² showed ohmic behavior over the current range of $10\text{--}1000\text{ }\mu\text{A}$, and the resistivity calculated from the slope of the line was $210\text{ }\mu\Omega\text{ cm}$ at 22°C . This is only about $60\text{ }\mu\Omega\text{ cm}$ higher than typical values for metallic

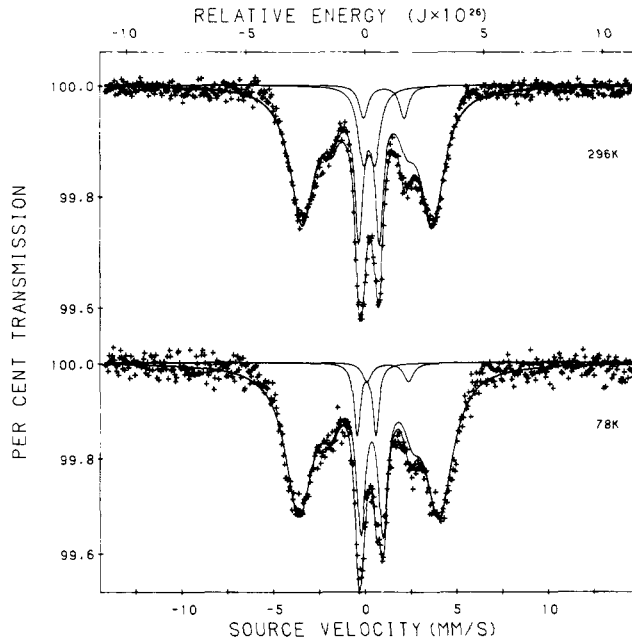


Figure 4. Mössbauer spectrum of iron-boride film deposited on iron-free aluminum foil and obtained at 296 and 78 K.

glasses and indicates that the integrity of the film is high and that the material is pure.^{13,14} Resistivity measurements were also made at a single current of 22 mA by using an apparatus with four needlelike contacts pressed into the film. This provided a rapid method for making survey measurements. For films prepared with a crucible to substrate distance of 3.5 cm, the resistivity varied 10% over the surface. Some of this variation was caused by edge effects in the measurements. Over a period of 2 months in air the resistivity of a typical film remained constant within an experimental error of $\pm 10\%$. As resistivity depends strongly on the extent of oxidation (see below), this shows that although the surface is subject to oxidation, the bulk of the film is protected.

Magnetic Properties. One of the advantages of working with iron-based films is that the Mössbauer technique can be used to obtain information on the local environments of the iron atoms as well as information on the magnetic ordering of the film. This allows the dependence of material structure as a function of preparative method to be examined at more than one size regime. Spectra of films deposited on iron-free aluminum foil obtained at 296 and 78 K are shown in Figure 4. The observed spectrum has a major component that can be fit with a sextet and two minor components that can be fit

(11) Fehlner, T. P.; Amini, M. M.; Stickle, W. F.; Pringle, O. A.; Long, G. J.; Fehlner, F. P. *Chem. Mater.* 1990, 2, 263.

(12) Valdes, L. B. *Proc. IRE* 1954, 42, 420.

(13) Johnson, W. L.; Tenhover, M. In *Glassy Metal: Magnetic, Chemical and Structural Properties*; Hasegawa, R., Ed.; CRC Press: Boca Raton, FL, 1983; p 65.

(14) Whittle, G. L.; Stewart, A. M.; Kaiser, A. B. *Phys. Status Solidi A* 1986, 97, 199.

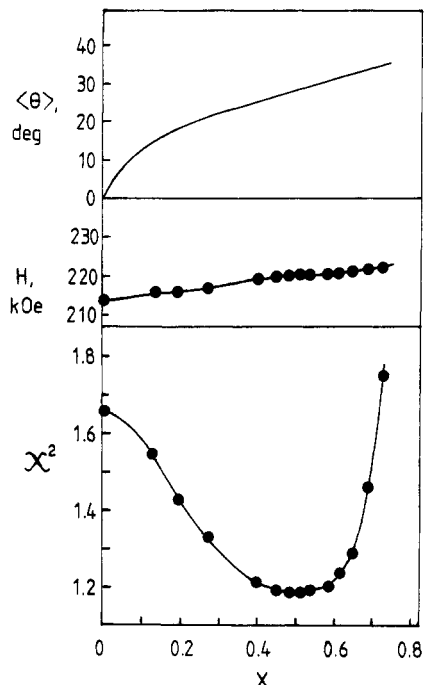


Figure 5. Variation of x^2 , the internal hyperfine field, H , and $\langle\theta\rangle$ with x for the Mössbauer spectrum shown in Figure 4 obtained at 296 K.

with doublets as shown by the solid lines in Figure 4. There is no evidence for the presence of α -iron in the film. The hyperfine parameters are listed in Table I. A number of reports of Mössbauer spectra of crystalline¹⁵ and amorphous $\text{Fe}_{75}\text{B}_{25}$ alloys have appeared,¹⁶⁻¹⁹ and the similarity of the major sextet component in our spectra to those reported earlier is evident. Clearly a magnetic phase is present, and the broad lines confirm the amorphous nature of the material. The Curie temperature of our material is above room temperature as is that of known $\text{Fe}_{75}\text{B}_{25}$ alloys.

There are, however, some real differences in the Mössbauer spectra of our material and spectra reported earlier. The most striking difference occurs in the orientation of the magnetic moments in the film. The intensity, x , of the 2/5 lines gives a direct measure of the orientation of the magnetic moments in the film relative to the direction of the Mössbauer γ -ray. For an x of 0, the film magnetization direction is perpendicular to the film plane and parallel to the γ -ray direction, whereas for an x of 4 the magnetization direction is in the film plane. Intermediate values correspond to a spatially averaged value of the magnetization direction for the entire sample.²⁰ The low intensity of the 2/5 sextet lines in Figure 4 demonstrates that the γ -ray is approximately parallel with the direction of magnetization, i.e., the magnetic moments have larger components normal to the plane of the foil. The area ratios (Table I) permit the mean orientation angle, $\langle\theta\rangle$, of the magnetic moments to be calculated. Because of the possibility of a correlation between the values of x , and hence $\langle\theta\rangle$, we have fit the spectra for various fixed values of x . The results shown in Figure 5 for the 296 K

spectrum indicate that the values of x , $\langle\theta\rangle$, and the internal field, H , are well determined. Very similar results were determined for the 78 K spectrum. The angle measured from the normal to the film is $28 \pm 3^\circ$ at 296 K and $29 \pm 3^\circ$ at 78 K which is similar to the 30° values reported earlier¹⁷ for electrolytically prepared films having the composition $\text{Fe}_{82}\text{B}_{18}$. In these electrolytic films preferential orientation of the magnetization normal to the film plane was attributed to the columnar film microstructure and the formation of ellipsoidal defects. Apparently, film growth in our case is also columnar. For a $\text{Fe}_{77}\text{B}_{23}$ sample produced by "electroless" methods a random orientation of the magnetic moments was observed.¹⁷ Further, most FeB amorphous alloys prepared by rapid quenching^{16,18} have the magnetization axis lying in the sample plane.²¹ Hence, even though the materials produced by rapid quenching of $\text{Fe}_{75}\text{B}_{25}$ melts or thermal decomposition of $\text{HFe}_3(\text{CO})_9\text{BH}_4$ are compositionally the same, the deposition product from the molecular precursor yields a material with significantly different magnetic properties.

As indicated in Table I and Figure 5, the internal hyperfine field for the magnetic sextet is 220 ± 2 kOe at 296 K and 237 ± 3 kOe at 78 K. These values indicate that the internal field, H , is about 10–20 kOe lower in our film than that reported for similar films,¹⁷ which in turn are about 20 kOe lower than those reported for bulk materials of similar composition.¹⁸ It is known that the hyperfine field decreases and the isomer shift increases with increasing metalloid concentration.¹⁸ Hence, part of the difference may be ascribed to small differences in composition. Alternatively, the incorporation of hydrogen into a film prepared by "electroless" deposition has been suggested as a possible cause of the low observed hyperfine fields. We cannot eliminate the possibility that low levels of carbon and oxygen or unknown amounts of hydrogen reduce the hyperfine field values in our films. It is clear, however, that the observed field strength for our film makes it unlikely that the iron content is higher than 75% and that the film is, in fact, essentially $\text{Fe}_{75}\text{B}_{25}$.

As there is a relationship between the iron hyperfine fields and the number of metalloid near neighbors, the distribution of magnetic hyperfine fields [$P(H)$] contains information on the metalloid structure.²² For example, the shape and width of the distribution has been found to be nearly independent of concentration for Fe–B metallic glasses, thereby suggesting a highly correlated structure.²³ In contrast to other iron-based amorphous alloys, glasses formed with boron tend to exhibit symmetric $P(H)$ distributions.²⁴ Thus, to compare our film with similar materials, we have fit the spectra and calculated a $P(H)$ distribution. Because there is a high correlation of $\langle\theta\rangle$ with the $P(H)$ distribution, the value of $\langle\theta\rangle$ has been constrained to 29° in these fits. The results are given in Figure 6, where it may be seen that the distribution is significantly asymmetrical or bimodal. The largest peak in the distribution centered at ≈ 225 kOe at 296 K and ≈ 250 kOe at 78 K is very similar to that found previously for $\text{Fe}_{75}\text{B}_{25}$ films prepared electrolytically and by rapid quenching methods.^{17,23,25} However, our film also exhibits a substantial number of iron atoms with rather small in-

(15) Choo, W. K.; Kaplow, R. *Metall. Trans. A* 1977, 8A, 417.
 (16) Vincze, I.; Van der Woude, F. *J. Non-Cryst. Solids* 1980, 42, 1980.
 (17) Nikolov, S.; Valsyunene, Y.; Dragieva, I. *Solid State Commun.* 1988, 66, 71.
 (18) Kemeny, T.; Vincze, I.; Fogarassy, B.; Araiza, S. *Phys. Rev. B* 1979, 20, 476.
 (19) Chien, C. L.; Unruh, K. M. *Phys. Rev. B* 1981, 24, 1556.
 (20) Chien, C. L.; Hasegawa, R. *J. Appl. Phys.* 1976, 47, 2234. Hasegawa, R.; Chien, C.-L. *Solid State Commun.* 1976, 18, 913.

(21) Chien, C.-L.; Hasegawa, R. In *Amorphous Magnetism*; Levi, R. A.; Hasegawa, R.; Eds.; Plenum Press: New York, 1977; p 289.
 (22) Vincze, I.; Boudreaus, D. S.; Tegze, M. *Phys. Rev. B* 1979, 19, 4896.
 (23) Vincze, I.; Kemeny, T.; Arajo, S. *Phys. Rev. B* 1980, 21, 937.
 (24) Durand, J. In *Glassy Metal: Magnetic, Chemical and Structural Properties*; Hasegawa, R., Ed.; CRC Press: Boca Raton, FL, 1983; p 65.
 (25) Chien, C. L.; Musser, D.; Gyorgy, E. M.; Sherwood, R. C.; Chem. H. S.; Luborsky, R. E.; Walter, J. L. *Phys. Rev. B* 1979, 20, 283.

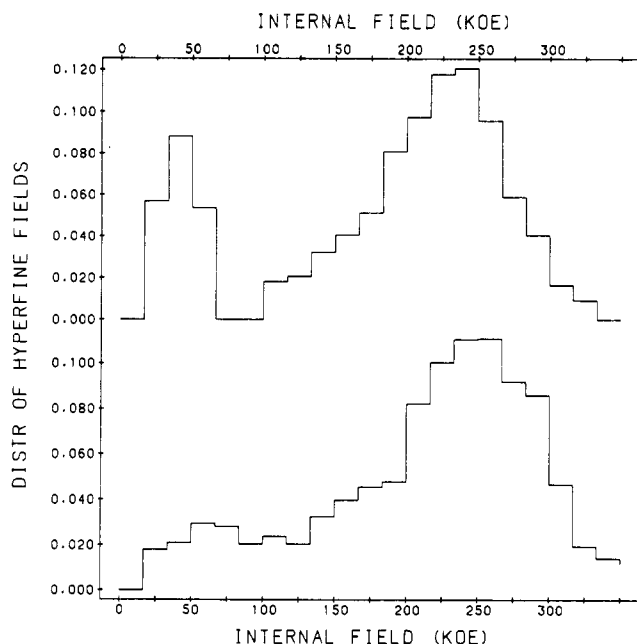


Figure 6. $P(H)$ distribution calculated for the Mössbauer spectra in Figure 4 obtained at 296 (top) and 78 K (bottom). The 3–5% by area high-spin iron(II) doublet has been subtracted from the spectral data prior to this $P(H)$ fit.

ternal fields, suggesting environments with larger numbers of non-iron nearest neighbors.²⁶ This may be a consequence of significant differences in the film structure as compared to films prepared by other techniques, or the known impurities (C and O) may have a significant effect on the magnetic behavior. In the supposedly hydrogen-contaminated film prepared by “electroless” deposition,¹⁷ a symmetrical $P(H)$ distribution shifted to lower fields was observed. This plus the fact that impurity levels are low in our film suggests that the asymmetric distribution is due to structural differences associated with the method of formation. Hence, the low-temperature deposition of $\text{HFe}_3(\text{CO})_9\text{BH}_4$ produces materials with many similarities to $\text{Fe}_{75}\text{B}_{25}$ prepared by other methods but also with some detailed structural differences.

Oxidized Films. Once the surface oxidizes, the $\text{Fe}_{75}\text{B}_{25}$ films prepared as described above are stable in air. Repetitive studies of the same film over a period of a month revealed no systematic changes in the composition or the resistivity of the film. The self-limiting surface oxidation occurring on exposure to the atmosphere can be distinguished from oxidation that takes place during deposition. Film deposition in an apparatus with poorer base pressures (10^{-6} Torr) led to smokey black, dull films exhibiting oxygen contents of up to 50% and very high resistivities. Hence, the films described above could be prepared only in a high vacuum system (10^{-8} Torr) in which air and particularly water vapor could be kept at low enough levels such that the rate of oxidation was no longer competitive with the rate of deposition. Because the formation of the boride films from molecular ferraboranes was sensitive to oxidizing impurities, whereas other systems, e.g., nitrides,¹⁰ were not, we decided to explore some of the characteristics of the oxidation process. All the films we have prepared have very uniform compositions that are independent of the extent of oxidation. Hence, the possibility exists that this reactivity could be used to form ternary films with specified extents of conversion and with appropriately modified properties.

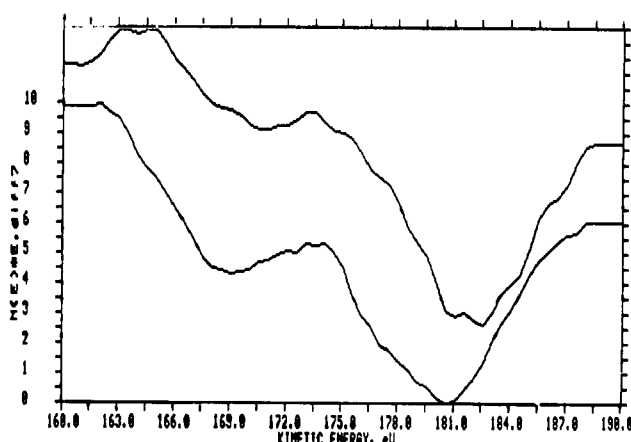


Figure 7. Auger KLL lines ($dN(E)/E$) for boron showing the line due to oxidized boron (169 eV) and boride (180 eV). The upper spectrum was obtained with continuous sputtering (1 kV, $4 \times 4 \text{ mm}^2$) whereas the lower spectrum was obtained ca. 10 min after sputtering for 1 min (5 kV, $1 \times 1 \text{ mm}^2$).

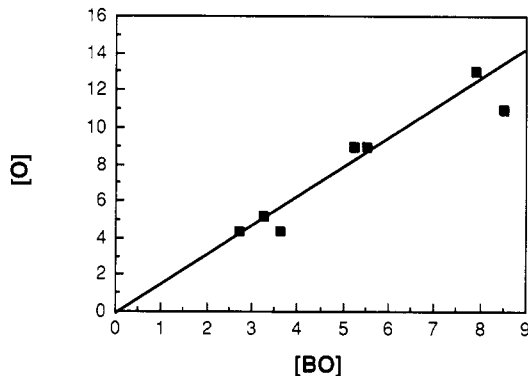


Figure 8. Plot of atom percent oxygen vs atom percent oxygen present as BO_x calculated from the ratio of the 169- and 180-eV boron Auger lines (see text).

The sensitivity of a clean $\text{Fe}_{75}\text{B}_{25}$ film to oxidation in a high vacuum environment is illustrated in Figure 7. The top spectrum, which was acquired during continuous, mild sputtering, shows an oxygen content of 9%. The main boron peak (180 eV) is due to boride, whereas the small peak at lower in kinetic energy (170 eV) is due to oxidized boron.²⁷ The lower spectrum was acquired from the same sample area ca. 10 min after sputtering away the surface layer. Reaction with the residual gas in the spectrometer (10^{-9} Torr of total pressure) leads to an increase in the peak due to oxidized boron, and there is a corresponding increase in the intensity of the oxygen line, i.e., the oxygen content increases from 9 to 18% in 30 min. The increase in the intensity of the Auger line from oxidized boron shows that the increasing oxygen content is not just due to an adsorbed oxygen-containing species but rather is due at least in part to a chemical reaction at the surface. Considering the low base pressure of the spectrometer, the reaction must be a facile one indeed. Oxidation of metal borides under similar conditions has been observed previously.²⁸ The oxidation of the surfaces of metal borides has also been studied earlier by utilizing XPS, and the conclusions concerning the species present are similar to those for our films.^{29,30}

(27) Huntley, D. R.; Overbury, S. H.; Zehner, D. M.; Budai, J. D.; Brower, W. E., Jr. *Appl. Surf. Sci.* 1986, 27, 180.

(28) Wayda, A. L.; Schneemeyer, L. F.; Opila, R. L. *Appl. Phys. Lett.* 1988, 53, 361.

(29) Myhra, S.; Riviere, J. C. *J. Non-Cryst. Solids* 1988, 99, 244.

(30) Myhra, S.; Riviere, J. C.; Welch, L. S. *Appl. Surf. Sci.* 1988, 32, 156.

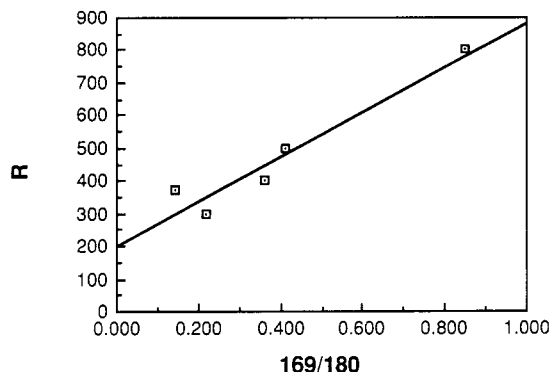


Figure 9. Plot of film resistivity ($\mu\Omega$ cm) vs extent of oxidation as measured from the ratio of the 169- and 180-eV boron Auger lines.

Since we can measure the total oxygen content and, from the two boron lines, distinguish between the boron present as boride and that present as oxidized boron, we can measure the stoichiometry of the oxide, i.e.

$$[\text{O}]_{\text{total}} = [\text{O}]_{\text{free}} + x[\text{O}]_{\text{BO}}$$

where x is the ratio of oxygen to boron in the oxide. As shown in Figure 8 a plot of $[\text{O}]_{\text{total}}$ vs $[\text{O}]_{\text{BO}}$, for a number of films with differing oxygen contents, is linear. The zero intercept suggests all the oxygen in this concentration range is bound as a boron oxide. The slope of ≈ 1.5 suggests that the stoichiometry of the oxide is B_2O_3 . Data from the $\text{Fe}_{80}\text{B}_{20}$ films can be incorporated into the same plot. At oxygen contents higher than 20% the curve is no longer linear, and the discontinuity correlates with the visible changes in color and reflectivity of the film. For oxygen contents below 20–30% all the boron can be converted to B_2O_3 in the $\text{Fe}_{80}\text{B}_{20}$ and $\text{Fe}_{75}\text{H}_{25}$ films, but for higher oxygen contents oxidation must seriously disrupt the metal–metal bonding network. The identity of the oxidizing species is not known; however, as the levels of H_2O vapor are an order of magnitude higher than those of O_2 , it seems likely that the former is the active species. Although the molecular cluster $\text{HFe}_3(\text{CO})_9\text{BH}_4$ is not itself sensitive to water vapor, after one or more CO ligands are removed, the reactivity of the B–H bond toward hydrolysis may well be greatly enhanced.

A more quantitative measure of the change in film properties comes from resistivity measurements as a function of the extent of oxidation of the boron. In Figure 9 resistivities measured by the four-point probe method are plotted vs the ratio of the intensities of the Auger signals due to oxidized boron and unoxidized boron. The highest point corresponds to an oxygen content of 11%. The resistivity increases approximately linearly with an intercept of $200 \mu\Omega$ cm which is close to the value measured for the purest film. It seems clear, then, that with the appropriate control of the atmosphere Fe–B–O films of uniform composition can be constructed.

Discussion

The main objective of this study was to demonstrate that the stoichiometry of the core of a transition metal–main-group atom molecular cluster can be deposited as a material of the same stoichiometry under mild conditions. Although the analytical data on the film composition does

not permit the first question to be answered as precisely as one would desire, it is clear that films with compositions approaching $\text{Fe}_{75}\text{B}_{25}$ can be reproducibly formed at relatively low temperatures on several substrates. The magnetic properties show that the local as well as long-range structure of the material is independent of the method of preparation but that the direction of magnetization relative to the film plane depends on the preparative method and, presumably, the film morphology. Hence, the molecular precursor route may be advantageous in growing films with special properties.

The facile oxidation of the Fe_3B films during deposition suggests a novel route to ternary materials. That is, a molecular precursor such as a transition metal and a main-group atom cluster can be used to fix the ratio of two elements, whereas a rapid reaction of the precursor during deposition with the source of another element introduces the third element. This would result in the formation of compositionally uniform films with properties that could be adjusted by varying the content of the third element in the film. This work demonstrates the feasibility of this idea for oxygen as the third element. Indeed one notes that the growth of oxide and semiconductor films are of significant interest.³¹ The approach might well be successful with other elements besides oxygen.

There are a wide variety of metallaboranes that have been prepared and characterized. They range from boron-rich to metal-rich systems.³² As pointed out by Lipscomb,³³ these compounds constitute a significant source of new solid-state borides with as yet unknown properties. This suggestion, of course, requires a method for translating the molecular units into the solid state without their destruction. For two metal-rich metallaboranes we have now shown that the existence of a low activation energy decomposition pathway permits the construction of known amorphous materials from the Fe_3B and Fe_4B units contained within the $\text{HFe}_3(\text{CO})_9\text{BH}_4$ and $\text{HFe}_4(\text{CO})_{12}\text{BH}_2$ molecules.

Acknowledgment. The support of the Army Research Office (Contract DAAL03-86-K-0136, TPF), the National Science Foundation (CHE87-01413, TPF), and the donors of the Petroleum Research Fund, administered by the American Chemical Society, are gratefully acknowledged. We thank Xiangsheng Meng for providing the samples of $\text{HFe}_3(\text{CO})_9\text{BH}_4$. T.P.F. thanks Prof. M. Lagally, A. Lefkow, and Dr. Ngoc C. Tran of the Thin Film Institute and Prof. D. F. Gaines, Dr. J. Wermer, and Prof. W. J. Pietro of the Chemistry Department of the University of Wisconsin for their assistance in carrying out part of this work and their hospitality during the tenure of a Guggenheim Fellowship.

Registry No. $\text{HFe}_3(\text{CO})_9\text{BH}_4$, 91128-40-4; $\text{B}_{25}\text{Fe}_{75}$, 67760-50-3.

(31) Kern, W.; Ban, V. S. In *Thin Film Processes*; Vossen, J. L., Kern, W., Eds.; Academic Press: New York, 1978; Chapter III-2.

(32) See: Grimes, R. N., Ed. *Metal Interactions with Boron Clusters*; Plenum Press: New York, 1982. Gilbert, K. B.; Boocock, S. K.; Shore, S. G. *Comp. Organomet. Chem.* 1982, 6, 879. Grimes, R. N. *Comp. Organomet. Chem.* 1982, 1, 459. Greenwood, N. N. *Chem. Soc. Rev.* 1984, 13, 353. Housecroft, C. E.; Fehlner, T. P. *Adv. Organomet. Chem.* 1982, 21, 57. Kennedy, J. D. *Prog. Inorg. Chem.* 1984, 32, 964. Kennedy, J. D. *Prog. Inorg. Chem.* 1986, 34, 211. Housecroft, C. E. *Polyhedron* 1987, 6, 1935. Fehlner, T. P. *New. J. Chem.* 1988, 12, 307, and references therein.

(33) Lipscomb, W. N. *J. Less Common Met.* 1981, 82, 1.